JOURNAL OF VIROLOGY, Mar. 2002, p. 2054–2061 Vol. 76, No. 5
0022-538X/02/$04.00+0 DOI: 10.1128/JVI.76.5.2054–2061.2002

Pathogenesis of Herpes Simplex Virus Type 2 Virion Host Shutoff (*vhs*) Mutants

Tracy J. Smith,[1] Lynda A. Morrison,[2] and David A. Leib[1,3]*

Departments of Ophthalmology and Visual Sciences[1] and Molecular Microbiology,[3] Washington University School of Medicine, St. Louis, Missouri 63110, and Department of Molecular Microbiology and Immunology, Saint Louis University School of Medicine, St. Louis, Missouri 63104[2]

Received 17 September 2001/Accepted 28 November 2001

During lytic infection, the virion host shutoff (vhs) protein mediates the rapid degradation of mRNA and the shutoff of host protein synthesis. In vivo, herpes simplex virus type 1 (HSV-1) mutants lacking *vhs* activity are profoundly attenuated. Homologs of *vhs* exist in all of the neurotropic herpesviruses, and the goal of this study was to determine the virulence of HSV-2 mutants lacking vhs. Two HSV-2 recombinants were used in this study: 333-*vhs*B, which has a *lacZ* cassette inserted into the N terminus of *vhs*, and 333d41, which has a 939-bp deletion in *vhs*. As expected, both 333-*vhs*B and 333d41 failed to induce the cellular RNA degradation characteristic of HSV. Corneal, vaginal, and intracerebral routes of infection were used to study pathogenesis. Both viruses grew to significantly lower titers in the corneas, trigeminal ganglia, vaginas, dorsal root ganglia, spinal cords, and brains of mice than wild-type and rescue viruses, with a correspondingly reduced induction of disease. Both viruses, however, reactivated efficiently from explanted trigeminal ganglia, showing that *vhs* is dispensable for reactivation. The lethality of 333d41 following peripheral infection of mice, however, was significantly higher than that of 333-*vhs*B, suggesting that some of the attenuation of 333-*vhs*B may be due to the presence of a *lacZ* cassette in the *vhs* locus. Taken together, these data show that *vhs* represents an important determinant of HSV-2 pathogenesis and have implications for the design of HSV-2 recombinants and vaccines.

Herpes simplex virus (HSV) induces a rapid destabilization of mRNA due to the product of the viral UL41 gene, known as the virion host shutoff (vhs) protein. This 58-kDa phosphoprotein, packaged within the tegument of the virus, is released directly into the cytoplasm upon infection, where it immediately begins to degrade mRNA prior to any viral gene expression (7, 23). Recent studies have demonstrated that vhs has endoribonucleolytic activity near the 5′ end of target mRNA (3, 4, 15), which requires a cellular factor (18) but no other viral proteins (14, 20). Viruses containing mutations within any of the four conserved domains in the UL41 gene do not cause RNA destabilization upon infection (8, 22, 23, 25). Such mutants are viable in cell culture, and the effect of *vhs* deletion on viral replication in tissue culture is minimal (22).

The genomes of HSV type 1 (HSV-1) and HSV-2, varicella-zoster virus, equine herpesvirus, and pseudorabies virus all have homologs of *vhs* (1). The conservation of *vhs* in these and other neurotropic alphaherpesviruses and its apparent absence in beta- and gammaherpesviruses suggest that *vhs* plays a role in neuropathogenesis, although the role of *vhs* in this context has only been studied in HSV-1. The goal of this study was therefore to examine the contribution of *vhs* to the pathogenesis of HSV-2.

The pathogenesis of HSV-1 and HSV-2 infections in humans and animal models has some general similarities and some important differences. HSV-1 is primarily associated with orolabial lesions, stromal keratitis, and occasionally encephalitis (27). HSV-2 primarily causes genital infections but is also capable of necrotizing stromal keratitis, encephalitis, meningitis, and neonatal ophthalmic, and neurologic complications in infants surviving infection (27, 32). In animal models, HSV-2 is significantly more neurovirulent than HSV-1 by all routes of infection (12, 16, 26).

HSV-1 mutants lacking *vhs* function have a significantly reduced capacity to replicate in the cornea, trigeminal ganglia, and brains of mice and show impaired establishment and reactivation from latency in a murine eye model of latency and pathogenesis (29–31). UL41 mutant viruses, however, remain highly immunogenic, suggesting that deletion of *vhs* may be a useful property for live-attenuated herpesvirus vaccines (10, 34, 35). The *vhs* proteins of HSV-1 and HSV-2 are 87% identical at the amino acid level, although the shutoff activity of HSV-2 is significantly faster than that of HSV-1 (5, 6, 13). The kinetics of *vhs* activity, however, do not correlate with virulence, since replacement of the *vhs* from HSV-1 with the higher-activity *vhs* allele from HSV-2 fails to alter the virulence of the HSV-1 recombinant (26). In addition, *vhs* from HSV-2 in combination with ICP47 has been shown to block antigen presentation by class I major histocompatibility complex (MHC) (33). It was therefore of interest to assess the contribution of *vhs* to the pathogenesis of HSV-2.

In this study, two HSV-2 recombinants lacking *vhs* activity were tested in ocular and genital models of infection in mice. The data show that these viruses are attenuated and that *vhs* represents an important determinant of HSV-2 pathogenesis. In addition, we show that the presence of *lacZ* in the viral genome can complicate interpretation of the phenotypes of

* Corresponding author. Mailing address: Department of Ophthalmology and Visual Sciences, Washington University School of Medicine, Box 8096, 660 S. Euclid Ave., St. Louis, MO 63110. Phone: (314) 362-2689. Fax: (314) 362-3638. E-mail: Leib@vision.wustl.edu.

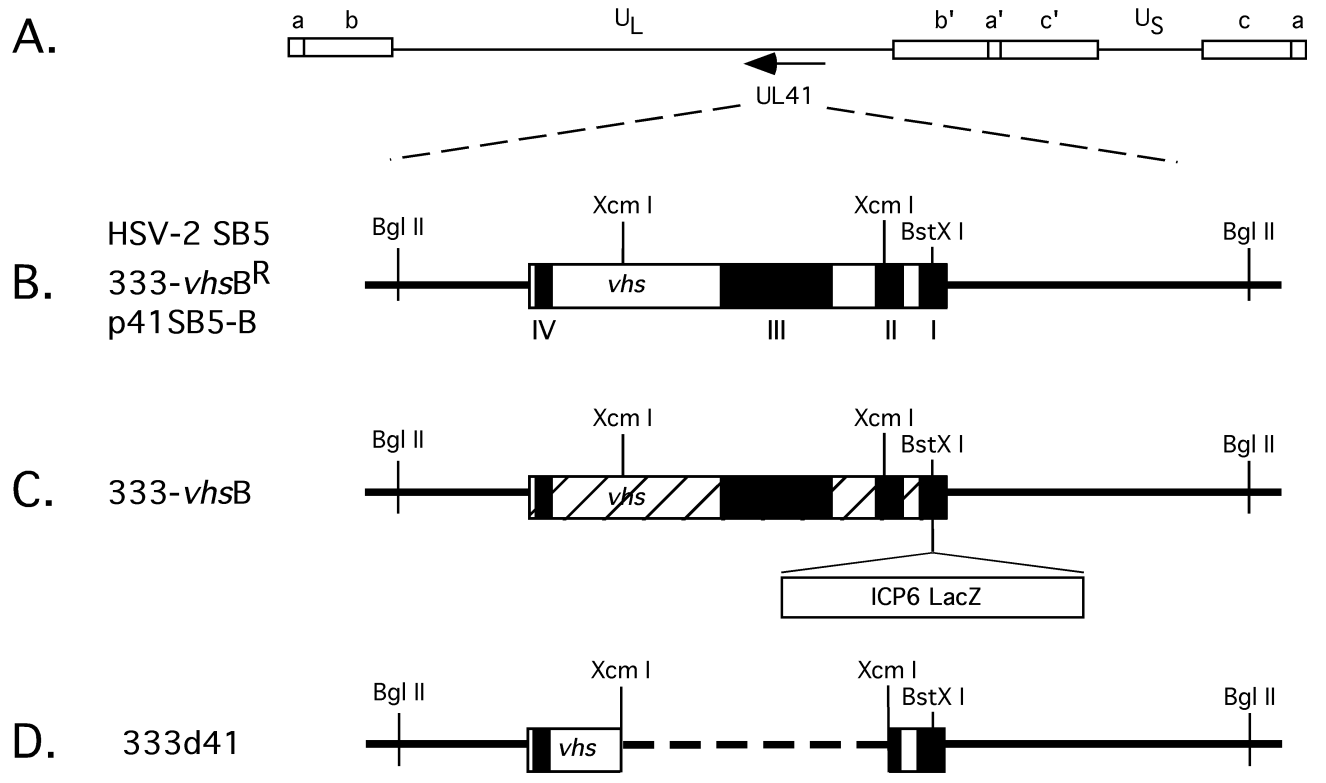

FIG. 1. Maps of *vhs* (UL41) ORF and viral mutants used in this study. (A) Prototypical arrangement of the HSV-1 genome, showing unique long (U_L) and unique short (U_S) segments flanked by internal (a′, b′, and c′) and terminal (a, b, and c) repeats. The direction of transcription for UL41 is indicated by the arrow. (B) Expanded view of the UL41 region, showing selected restriction enzyme sites and the conserved sequence domains among the *vhs* homologs (I to IV, black boxes) for HSV-2 SB5, a plaque-purified strain of 333, and the marker-rescued virus 333-*vhs*B^R. The *Bgl*II sites delineate the limits of the UL41 region within the plasmid p41SB5-B, used for transfections and as a probe in Southern blots. (C) Map of the UL41 region for 333-*vhs*B, showing insertion of an ICP6 *lacZ* expression cassette into a *Bst*XI restriction site of the UL41 ORF. Hatched areas represent predicted out-of-frame regions for UL41. (D) Map of the UL41 region of an HSV-2 deletion virus, 333d41, showing an *Xcm*I 940-bp deletion within the UL41 ORF.

HSV mutants. These data have implications for the design of HSV recombinants and vaccines.

MATERIALS AND METHODS

Cells and viruses. African green monkey kidney (Vero) cells were maintained at 5% CO_2 in a humidified incubator at 37°C and propagated as described previously (21). Growth and plaque assays of all viruses were carried out as described previously (21). SB5, a plaque-purified stock of HSV-2 strain 333, was obtained from the American Type Culture Collection (VR-2546). 333-*vhs*B was a gift from Jim Smiley (University of Edmonton, Edmonton, Alberta, Canada). It was constructed by disrupting the UL41 open reading frame (ORF) in HSV-2 strain 333 DNA by insertion of an expression cassette consisting of the HSV-1 ICP6 promoter driving the *lacZ* gene (11) into a *Bst*X1 restriction site at codon 30 of the *vhs* ORF (33). Marker rescue to produce 333-*vhs*B^R was accomplished by cotransfecting p41SB5-B (a plasmid with a *Bgl*II genomic clone of HSV-2 333 containing UL41) and 333-*vhs*B infectious DNA. Progeny were screened by the selection of white plaques and analyzed by Southern blotting for an appropriately altered *Bam*HI digestion pattern. Virus was plaque purified three times and grown to a high-titered stock.

An internal *Xcm*I fragment was excised from the *vhs* coding sequence in p41SB5-B to construct pdl41SB5-B. This was cotransfected with infectious 333-*vhs*B DNA to generate the virus 333d41. White plaque progeny were analyzed by Southern blotting and grown to a high-titered stock as described above. Lipofectamine (Life Technologies, catalog no. 18324–012; Rockville, Md.) was used in all transfections with a modification of the procedure recommended by the manufacturer. Briefly, 1 μg each of plasmid and infectious DNA in a volume of 100 μl of serum-free medium were mixed gently with 12 μl of Lipofectamine reagent diluted in a volume of 100 μl of serum-free medium. After incubating at room temperature for 30 min, 0.8 ml of serum-free medium was added to the mixture and overlaid onto 60% confluent Vero cell monolayers in 35-mm tissue culture plates rinsed with serum-free medium. After a 4-h incubation at 37°C in a 5% CO_2 incubator, 2 ml of medium containing 10% serum was added. The incubation was continued for another 18 to 24 h, at which time the medium was replaced with 3 ml of fresh medium containing 10% serum. Southern blot analyses of viral DNA were performed as described previously (24), using random primed ^{32}P-labeled p41SB5-B.

Northern blot analysis and mRNA degradation assay. Total cytoplasmic RNA was prepared from monolayer cultures of infected or mock-infected Vero cells as described previously (23). Monolayer cultures of 5×10^5 to 5×10^6 cells were mock infected or infected at a multiplicity of infection (MOI) of 20 with SB5, 333-*vhs*B, 333d41, or 333-*vhs*B^R in the presence of 10 μg of actinomycin D per ml. Mock-infected plates received Vero cell lysate only. Cytoplasmic RNAs were harvested at 2, 4, and 6 h postinfection and analyzed for mRNA degradation by Northern blot analysis, probing for glyceraldehyde-3-phosphate dehydrogenase (GAPDH) (9, 31). Filters were first probed for GAPDH, stripped, and then reprobed for the 28S ribosomal subunit. Phosphoimages were scanned on a Molecular Dynamics Storm 860 Phosphorimager and quantified. The level of GAPDH for 28S-normalized mock-infected cells was set at 100% and compared with the 28S-normalized GAPDH values of virus-infected cells.

Animal procedures. Replication in the corneas and trigeminal ganglia was evaluated in CD-1 female mice (weight, 21 to 25 g; Charles River Breeding Laboratories, Inc., Kingston, N.Y.). Mice were anesthetized intraperitoneally with ketamine (87 mg/kg) and xylazine (13 mg/kg). Corneas were bilaterally scarified with 10 interlocking strokes with a 25-gauge needle and inoculated with 5 μl of 2×10^6 PFU of virus per eye. Lids were massaged together briefly to promote adsorption of virus. Eye swab material (17) and trigeminal ganglion homogenates (26) were prepared as described previously and assayed for virus by

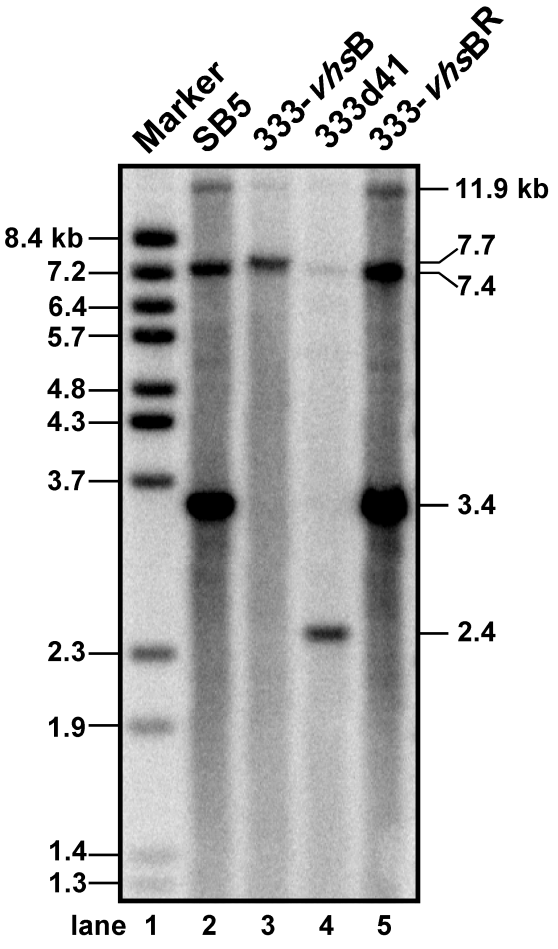

FIG. 2. Southern blot analysis of SB5, 333-*vhs*B, 333d41, and 333-*vhs*B^R, using p41SB5-B as a probe (see Fig. 1 for UL41 region delineated by this plasmid). Positions of the fragments with the expected sizes resulting from a *Bam*HI digestion are indicated on the right (in kilobases) and indicate that the UL41 region of each virus was as predicted: 11.9-, 7.4-, and 3.4-kb fragments for SB5 and 333-*vhs*B^R, 11.9-, 7.7-, and 7.4-kb fragments for 333-*vhs*B, and 11.9-, 7.4-, and 2.4-kb fragments for 333d41. Sizes of *Bst*EII-digested bacteriophage lambda DNA fragments are indicated on the left.

standard plaque assay. For intracerebral infections, anesthetized mice received 20 μl of virus inoculation containing 5×10^2 PFU. At the indicated times postinfection, brains were harvested, weighed, and stored in medium containing 3-mm glass beads at −80°C. Individual brains were homogenized and assayed for virus on Vero cells as previously described (31). Reactivation of virus from latency was examined by removing trigeminal ganglia 28 days postinfection as previously described and assaying them for infectious virus on new Vero cell monolayers (26). For lethality data, time to death was recorded.

Viral replication in the vagina and spinal cord was evaluated in 6-week-old BALB/c female mice (National Cancer Institute, Frederick, Md.) Seven and one days prior to infection, mice were injected subcutaneously in the scruff of the neck with depoprovera (3 mg per mouse in a 100-μl volume). Mice were anesthetized with nembutal (70 mg/kg of body weight), swabbed intravaginally once with a calcium alginate swab (Puritan, Guilford, Maine), and intravaginally inoculated with 2×10^6 PFU of SB5 or 333-*vhs*B in a volume of 5 μl. The vaginal mucosa was swabbed twice on day 2 after infection, and swabs were placed together into 1 ml of phosphate-buffered saline. Spinal cords were dissected, and the lower spinal cord was isolated and placed in assay medium containing glass beads. Vaginal swabs and spinal cord homogenates were assayed for virus by standard plaque assay.

RESULTS

Construction and comparison of UL41 mutants. Two HSV-2 *vhs* null viruses were used in this study (Fig. 1). The first, 333-*vhs*B (provided by Jim Smiley, University of Edmonton), is a *vhs* null virus containing a *lacZ* expression cassette driven by the HSV-1 ICP6 gene promoter inserted into conserved domain I of UL41 (1). This virus was marker rescued for this study to yield 333-*vhs*B^R. The second *vhs* null virus, 333d41, was constructed in the present study by excising 939 bp from the HSV-2 *vhs* ORF between two *Xcm*I restriction enzyme sites at codons 95 and 405. This mutation removes part of conserved domain II and all of domain III from *vhs* (1). Southern blot analysis probing with random-primed p41SB5-B yielded the predicted *Bam*HI fragments for the UL41 region for each of the viruses in this study (Fig. 2): 11.9-, 7.4-, and 3.4-kb fragments for SB5 and 333-*vhs*B^R (lanes 2 and 5, respectively), 11.9-, 7.7-, and 7.4-kb fragments for 333-*vhs*B (lane 3), and 11.9-, 7.4-, and 2.4-kb fragments for 333d41 (lane 4).

Measurement of *vhs* activity. The *vhs* mutants 333 -*vhs*B and 333d41 were examined for their capacity to degrade GAPDH in parallel with wild-type HSV-2 (SB5) and 333-*vhs*B^R. Monolayer cultures of Vero cells were mock infected or infected at an MOI of 20 with SB5, 333 -*vhs*B, 333d41, or 333-*vhs*B^R in the presence of actinomycin D (10 μg/ml) to evaluate degradation of finite pools of RNA induced by preformed tegument-derived vhs. In these assays the level of GAPDH for 28S-normalized, mock-infected cells was set at 100% and compared with the 28S-normalized GAPDH values of virus-infected cells. As expected, the RNA degradation induced by 333-*vhs*B and 333d41 was minimal compared to that with the wild-type or rescued viruses at all time points (Fig. 3A). RNA degradation was readily detectable at 2 h postinfection, with SB5 and 333-*vhs*B^R degrading to 20% of mock-infected levels, and 333-*vhs*B and 333d41 being almost 90% of mock-infected levels. At 6 h postinfection GAPDH RNA was barely detectable in SB5- and 333-*vhs*B^R-infected cells, while levels in 333-*vhs*B- and 333d41-infected cells remained at approximately 90% of the level of mock-infected cells. This graph represents the averaged percent GAPDH degradation levels of two to four independent experiments. A representative Northern blot showing the autoradiographic bands from GAPDH message and the 28S rRNA loading control is shown in Fig. 3B. These data demonstrate that 333-*vhs*B and 333d41 are phenotypically *vhs* null viruses and confirm that GAPDH degradation is dependent on an intact UL41 gene.

Replication in tissue culture. The growth kinetics of SB5, 333-*vhs*B, 333d41, and 333-*vhs*B^R were examined in Vero cells in a multistep growth curve. Consistent with previous observations, no differences were observed between the wild-type and *vhs* null viruses (Fig. 4). Also consistent with previous findings in HSV-1 *vhs* null viruses, 333-*vhs*B and 333d41 have small-plaque phenotypes (data not shown).

Replication in mice. The growth of 333-*vhs*B and 333d41 was examined in vivo in mouse corneas, trigeminal ganglia, vaginas, spinal cords, and brains. Acute viral replication in the cornea was analyzed on days 1 to 5 postinfection by corneal scarification and infection with 2×10^6 PFU per eye (Fig. 5A). Similar titers of 333-*vhs*B and 333d41 were found in the cornea but were 5- to 100-fold lower than the titers of SB5 or 333-*vhs*B^R

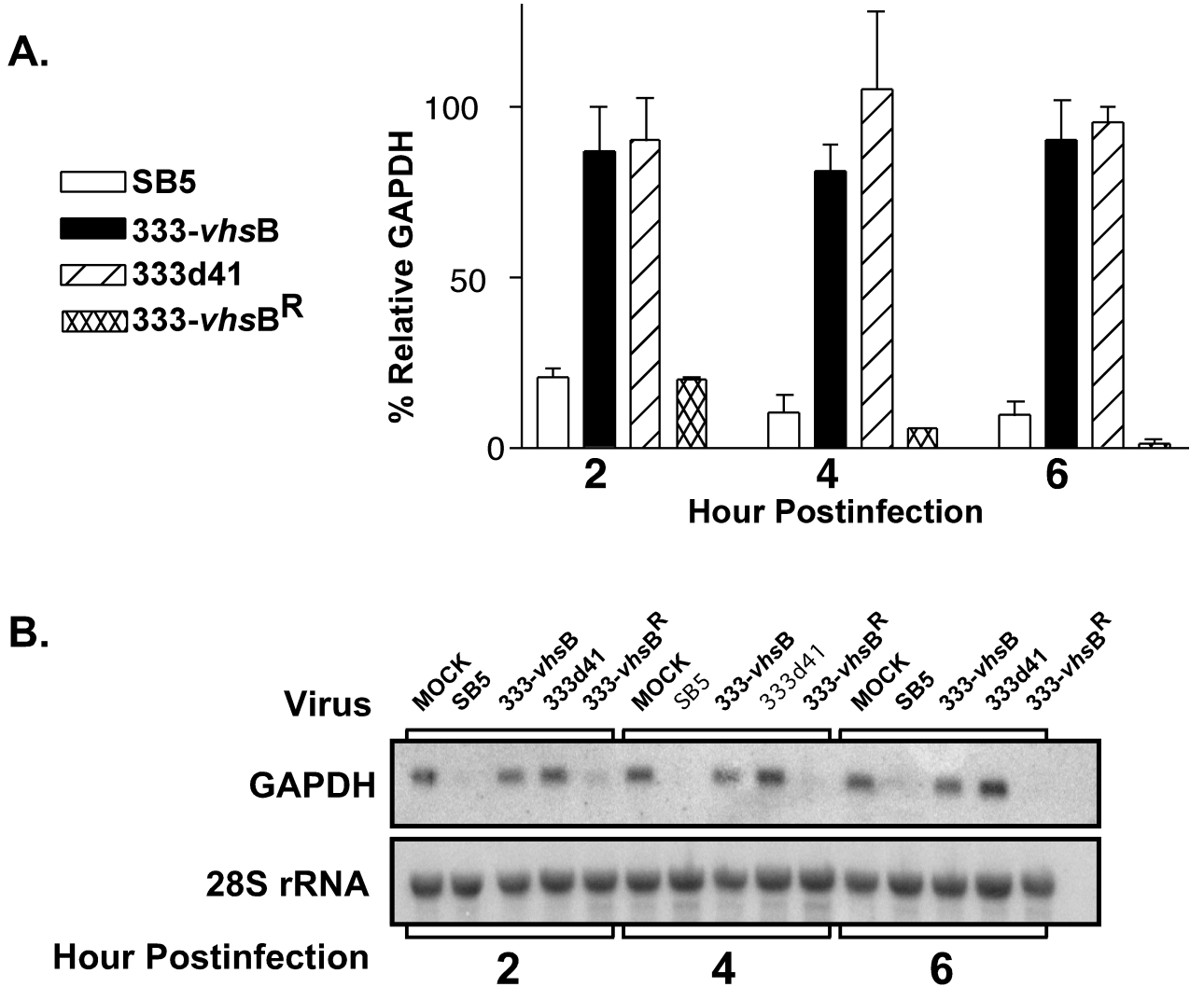

FIG. 3. RNA degradation assay by Northern blot analysis. Vero cells were mock infected or infected with SB5, 333-*vhs*B, 333d41, or 333-*vhs*B^R in the presence of actinomycin D (10 μg/ml), and cytoplasmic RNA was extracted. (A) Two independent experiments showing the average percent GAPDH RNA remaining relative to that in 28S rRNA-normalized, mock-infected cells. (B) Autoradiographic images show a representative Northern blot probed for GAPDH (top), and the same blot stripped and reprobed for the 28S ribosomal unit (bottom).

throughout the course of infection. The titers of 333-*vhs*B and 333d41 in trigeminal ganglia were significantly reduced compared to wild-type and rescued viruses 3 days postinfection, when peak titers are expected (Fig. 5B, $P < 0.0001$ for both by Student's *t* test).

Unexpectedly, especially since no significant difference in peripheral replication was observed between 333-*vhs*B and 333d41, the growth of 333-*vhs*B in the trigeminal ganglia was significantly reduced compared to 333d41 (Fig. 5B, $P = 0.0007$ by Student's *t* test). To address the concern that the lower replication in the nervous system of both mutant viruses was due to slight replication differences in the periphery, intracerebral injections were performed. Injection of 5×10^2 PFU per brain was sublethal, allowing survival of the mice to times when replication of the viruses could be measured easily. Replication of both 333-*vhs*B and 333d41 was significantly ($P < 0.0001$) compromised in brains relative to wild-type or marker-rescued viruses on both days 2 and 4 (Fig. 6). These data show that as for HSV-1, *vhs* of HSV-2 is critical for replication in the nervous system.

Having shown that the *vhs* mutants were attenuated in the ocular model, it was of interest to assess whether attenuation would also be apparent in the genital model, a more physiological route of infection for HSV-2. Acute replication of 333-*vhs*B, 333d41, and SB5 in the vagina and spinal cord was analyzed following intravaginal inoculation with 2×10^6 PFU. On day 2 postinfection, vaginal replication of 333-*vhs*B and 333d41 was significantly reduced relative to the growth of SB5 (Fig. 7A, $P < 0.0001$ by Student's *t* test). Likewise, a reduction in titer for both 333-*vhs*B- and 333d41-infected mice relative to SB5-infected mice was seen on day 4 postinfection in the lower spinal cord (Fig. 7B, $P < 0.0001$ by Student's *t* test). Correlative with data in the cornea and trigeminal ganglia, no significant difference in vaginal replication was observed between

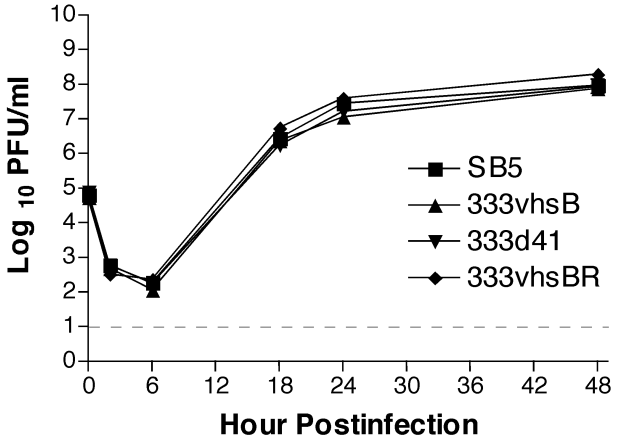

FIG. 4. Multistep growth kinetics of SB5, 333-*vhs*B, 333d41, and 333-*vhs*B^R in African green monkey kidney (Vero) cells at an MOI of 0.01. Each data point reflects the geometric mean PFU of virus per milliliter of sample ± standard error of the mean (SEM) of samples from two independent experiments performed in duplicate. Limit of detection, indicated by the dashed line, is 10 PFU/ml.

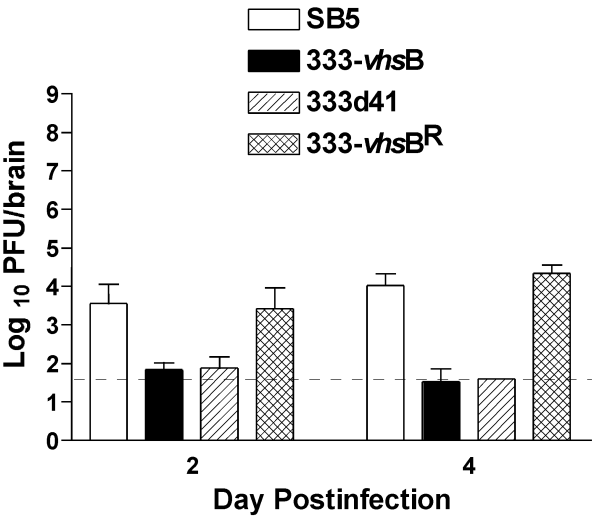

FIG. 6. Acute viral replication of SB5, 333-*vhs*B, 333d41, and 333-*vhs*B^R in mouse brain. Mice were infected intracerebrally with 5×10^2 PFU of virus. Each data point reflects the geometric mean PFU of virus per brain ± SEM from two independent experiments. In total, data points represent at least four brains per virus per day. The limit of detection, indicated by the dashed line, is 40 PFU/ml.

333-*vhs*B and 333d41, but the growth of 333-*vhs*B in the spinal cord was significantly reduced compared to that of 333d41 ($P < 0.05$ by Student's t test).

Collectively, these results demonstrate that HSV-2 *vhs* null mutants exhibit significantly reduced viral growth in both the mouse ocular and genital models. These results also suggest differences in the in vivo phenotypes of 333-*vhs*B and 333d41.

Lethality and reactivation. Following peripheral infection in mice, HSV-2 is highly neuroinvasive and neurovirulent. Using peripheral infection via the ocular route, we addressed whether *vhs* plays a role in neurovirulence in mice (Fig. 8, Table 1). At an inoculum of 2×10^6 PFU, 333-*vhs*B was significantly less neurovirulent than control viruses SB5 and 333-*vhs*B^R ($P = 0.0013$ and $P < 0.0001$, respectively, Student's t test). 333d41 was also significantly less virulent than control viruses ($P < 0.0001$ for both, Student's t test) but was significantly more virulent than 333-*vhs*B ($P = 0.0039$, Student's t test), consistent with its higher growth in trigeminal ganglia and spinal cords. At an inoculum of 2×10^3 PFU, 333-*vhs*B infection resulted in no lethality, while two of nine mice were killed by 333d41. Although the difference between the *vhs* mutants is not statistically significant at this dose ($P = 0.1451$, Student's t test), it follows the pattern of higher virulence for

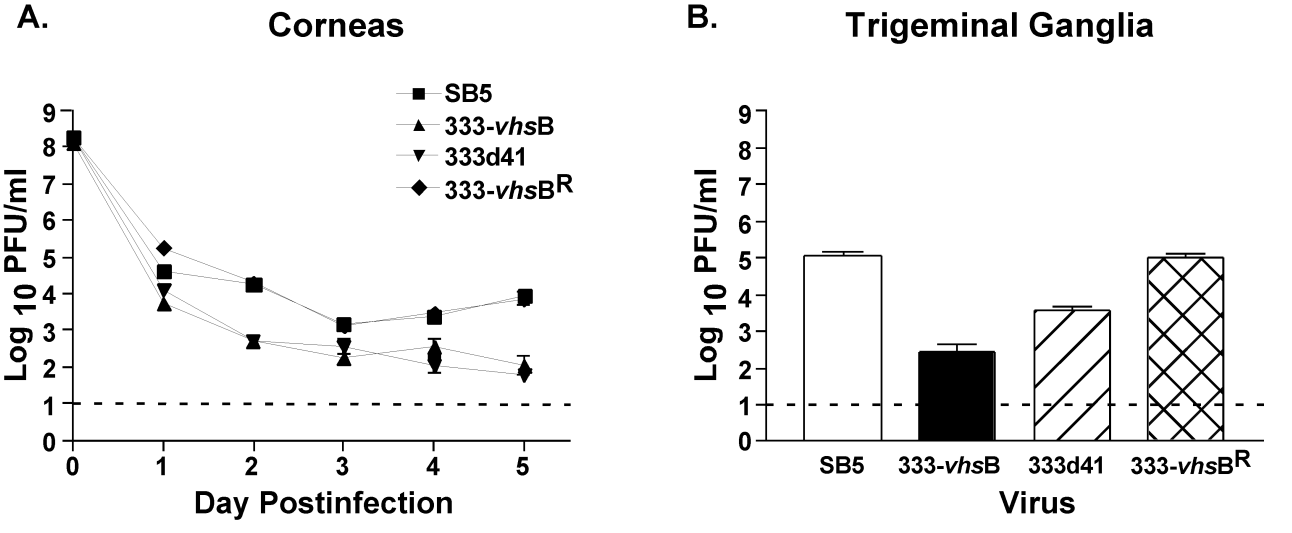

FIG. 5. Acute viral replication of SB5, 333-*vhs*B, 333d41, and 333-*vhs*B^R in mouse corneas (A) and trigeminal ganglia (B). Mice were infected via corneal scarification and inoculation with 2×10^6 PFU per eye. Each data point reflects the geometric mean PFU per milliliter of sample ± SEM of samples from at least two independent experiments. In total, data represent at least eight samples per virus per day. The limit of detection, indicated by the dashed line, is 10 PFU/ml.

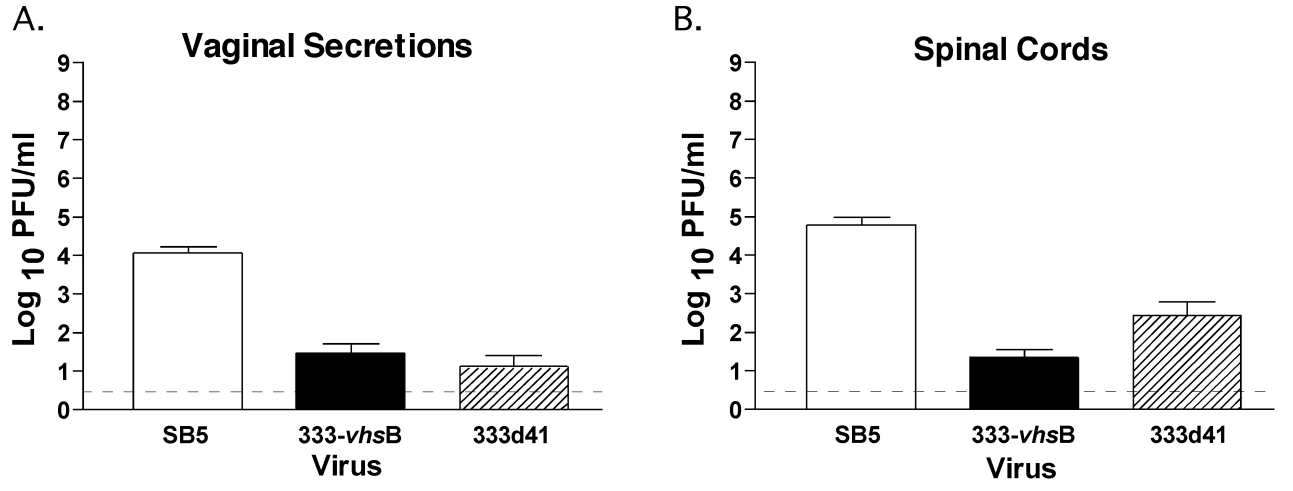

FIG. 7. Acute viral replication of SB5 and 333-*vhs*B in mouse vaginas (A) and spinal cords (B). Mice were infected by intravaginal inoculation with 2×10^6 PFU of virus. Each data point reflects the geometric mean PFU of virus per milliliter of sample ± SEM of samples from at least two independent experiments. In total, data represent at least seven mice per virus per day. The limit of detection, indicated by the dashed line, is 3 PFU/ml.

333d41. At this lower dose, control viruses had similar lethality ($P = 0.5270$, Student's t test), killing greater than 90% of mice (Fig. 8 and Table 1).

Reactivation frequencies from trigeminal ganglia were determined by explant cocultivation performed on day 28 postinfection. 333-*vhs*B reactivated efficiently (37 of 42 ganglia, Table 1) at the 2×10^6 PFU dose, but it was not possible to assess reactivation of 333d41 due to its high lethality. At 2×10^3 PFU per eye, the reactivation of 333-*vhs*B was seven of eight ganglia, and for 333d41 it was eight of eight ganglia. All but one wild-type-infected mouse and all rescued-virus-infected mice died at this dose. These data indicate that HSV-2 *vhs* null mutants are attenuated and, consistent with 333-*vhs*B reactivation at the higher dose, that *vhs* is not required for reactivation of HSV-2 from latently infected trigeminal ganglia. These data also provide evidence that 333-*vhs*B and 333d41, despite both being *vhs* null mutants, possess different neuroinvasiveness and virulence phenotypes.

DISCUSSION

Previous work in our laboratory demonstrated a critical role for *vhs* in the pathogenesis and latency of HSV-1 (26, 29–31). HSV-1 *vhs* mutants grow poorly in mice, have a reduced capacity to establish and reactivate from latency, and are very attenuated despite only minimal growth defects in cell culture. These viruses are, however, highly immunogenic and are effective as prophylactic and therapeutic vaccines in mice (10, 34, 35). Although the HSV-2 *vhs* null mutants tested in this study were significantly attenuated relative to wild-type and marker-

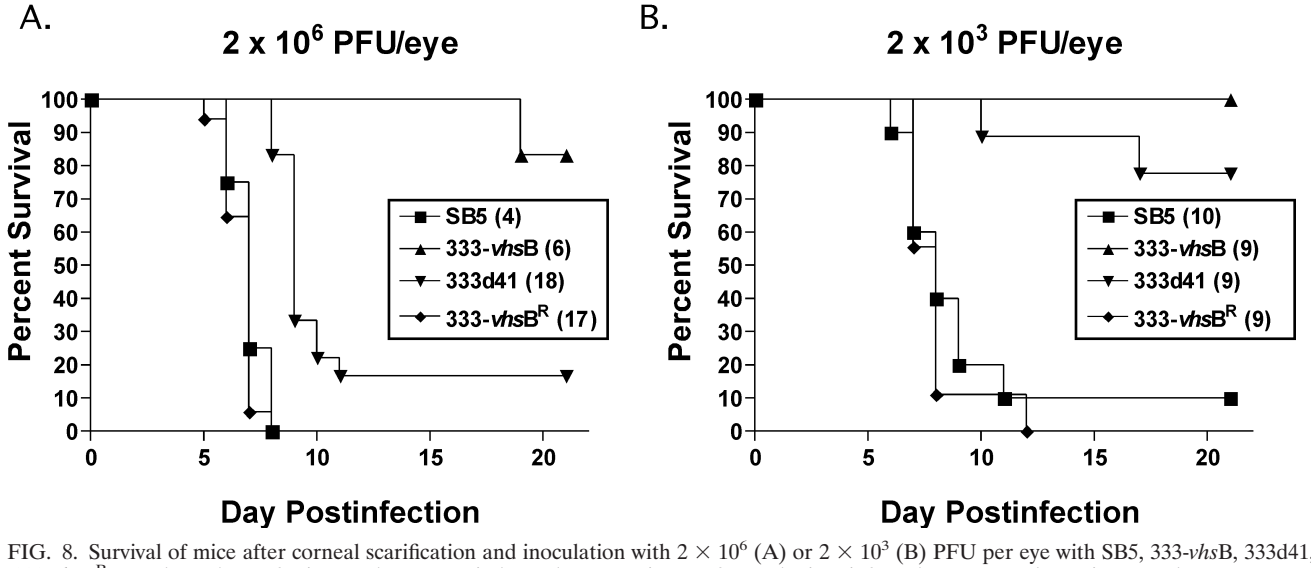

FIG. 8. Survival of mice after corneal scarification and inoculation with 2×10^6 (A) or 2×10^3 (B) PFU per eye with SB5, 333-*vhs*B, 333d41, or 333-*vhs*B^R. Total numbers of mice used over two independent experiments for each virus-infected group are shown in parentheses.

TABLE 1. Reactivation from latency and lethality data for SB5, 333-*vhs*B, 333d41, and 333-*vhs*B^R

Virus	Reactivation,[a] no. of ganglia yielding virus/no. assayed (%), at inoculum:		Lethality,[b] no. of mice dead/total (%), at inoculum:	
	2×10^6 PFU/eye	2×10^3 PFU/eye	2×10^6 PFU/eye	2×10^3 PFU/eye
585	ND[c]	2/2 (100)	20/20 (100)	9/10 (90)
333-*vhs*B	37/42 (88)	7/8 (88)	1/27 (4)	0/9 (0)
333d41	ND	8/8 (100)	15/18 (83)	2/9 (22)
333-*vhs*B^R	ND	ND	17/17 (100)	9/9 (100)

[a] Number of explanted latently infected trigeminal ganglia yielding virus per total number of ganglia assayed from all surviving mice. Percentage given in parentheses.
[b] Number of mice that died per total mice over 21 days postinfection. Percentage given in parentheses.
[c] ND, not determined.

rescued viruses, the impact of *vhs* deletion was less profound on the in vivo phenotype of HSV-2 than on that of of HSV-1. This relative lack of attenuation was observed regardless of whether the viruses were tested by the ocular route or the genital route, which is more appropriate for testing with HSV-2. In particular, 333d41 remained capable of significant growth in the nervous system and of causing lethal infection. This is not surprising, given the higher virulence of wild-type HSV-2 compared to HSV-1. Any evaluation of the utility of HSV-2 *vhs* deletion as a component of live-attenuated vaccines will therefore have to be performed in the context of replication-defective viruses, such as a virus lacking ICP8 (10, 19).

The mortality induced by 333-*vhs*B following peripheral infection and its replication within the trigeminal ganglia and spinal cords were significantly reduced compared to 333d41. We confirmed that this difference was not due to a secondary mutation by performing marker rescue to give 333-*vhs*B^R, whose phenotype was indistinguishable from that of wild-type virus. Such differences were not observed following intracerebral inoculations, although we deliberately used low inocula in these experiments to allow the mice to survive long enough to measure viral replication out to 4 days postinfection. Inoculations at higher doses would likely recapitulate the higher virulence and growth of 333d41 seen in other experiments, and such work is in progress.

Such experiments notwithstanding, these data underscore the role of *vhs* for promoting HSV growth in the nervous system. Recent studies have shown that insertion of a *lacZ* cassette can contribute to phenotypic changes in vivo (2, 28). These previous studies both used a human cytomegalovirus immediate-early promoter to drive expression of *lacZ*, and a strongly inducible promoter, ICP6 from HSV, drives *lacZ* expression in 333-*vhs*B (11). It is possible, therefore, that alterations in regional transcription and genome stability result from the insertion of these *lacZ* cassettes. It should also be noted that 333d41 might differ from 333-*vhs*B in expression of the undeleted portions of its *vhs* gene. If *vhs* has other functions in addition to RNA destabilization, this may be especially important. Alternatively, although less likely, *lacZ* may be acting as an immunogen to enhance clearance of the virus. Either way, these data suggest that in vivo phenotypes resulting from mutants containing a *lacZ* expression cassette should be interpreted with caution.

An important conclusion from the current study is that *vhs* is dispensable for reactivation. Reactivation of the *vhs* null mutants was close to 100%, even following inoculation with as little as 2×10^3 PFU per eye. Furthermore, efficient reactivation occurred despite reduced growth of the HSV-2 null mutants in the cornea and trigeminal ganglion. HSV-1 *vhs* null mutants, however, have a greatly reduced (up to 10,000-fold) ability to replicate in the nervous system and to establish and reactivate from latency compared to wild-type virus (30, 31). These previously published data used 5-day explant cocultivation assays, which are a qualitative rather than quantitative measure of reactivation. Recent experiments from our laboratory have used limiting dilutions of latently infected dissociated ganglia and daily sampling of supernatants out to 12 days. This method is both more sensitive and quantitative than those employed in previous studies and has shown that *vhs* activity is also dispensable for the reactivation of HSV-1 from explanted trigeminal ganglia (T. K. VanHeyningen and S. S. Strand, unpublished data).

The strong and exclusive conservation of *vhs* among the herpesviruses that establish latency in neurons implicates a requirement for the vhs protein in neuropathogenesis. Whether this requirement is at the level of promoting the establishment of latency, immune evasion (33), or a combination of both is unknown. It is also possible that *vhs* has functions in addition to destabilization of RNA that may impact upon the interactions between HSV and the nervous system, and the search for such functions is ongoing in our laboratory.

ACKNOWLEDGMENTS

We thank Jim Smiley for providing 333-*vhs*B. We also thank Skip Virgin and members of his laboratory for helpful discussions. The technical assistance of Li Zhu is gratefully acknowledged.

This study was supported by grants from the National Institutes of Health to David A. Leib (EY10707) and Lynda A. Morrison (CA75052). Core grant support from the National Eye Institute and Research to Prevent Blindness to the Department of Ophthalmology and a Robert E. McCormick Scholarship to David A. Leib are gratefully acknowledged.

REFERENCES

1. **Berthomme, H., B. Jacquemont, and A. Epstein.** 1993. The pseudorabies virus host-shutoff homolog gene: nucleotide sequence and comparison with alphaherpesvirus protein counterparts. Virology **193:**1028–1032.
2. **Clambey, E. T., H. W. T. Virgin, and S. H. Speck.** 2000. Disruption of the murine gammaherpesvirus 68 M1 open reading frame leads to enhanced reactivation from latency. J. Virol. **74:**1973–1984.
3. **Elgadi, M. M., C. E. Hayes, and J. R. Smiley.** 1999. The herpes simplex virus vhs protein induces endoribonucleolytic cleavage of target RNAs in cell extracts. J. Virol. **73:**7153–7164.
4. **Elgadi, M. M., and J. R. Smiley.** 1999. Picornavirus internal ribosome entry site elements target RNA cleavage events induced by the herpes simplex virus virion host shutoff protein. J. Virol. **73:**9222–9231.
5. **Everett, R. D., and M. L. Fenwick.** 1990. Comparative DNA sequence analysis of the host shutoff genes of different strains of herpes simplex virus: type 2 strain HG52 encodes a truncated UL41 product. J. Gen. Virol. **71:**1387–1390.

6. **Everly, D. N. J., and G. S. Read.** 1997. Mutational analysis of the virion host shutoff gene (UL41) of herpes simplex virus (HSV): characterization of HSV type 1 (HSV-1)/HSV-2 chimeras. J. Virol. **71:**7157–7166.
7. **Fenwick, M. L., and J. Clark.** 1982. Early and delayed shut-off of host protein synthesis in cells infected with herpes simplex virus. J. Gen. Virol. **61:**121–125.
8. **Fenwick, M. L., and R. D. Everett.** 1990. Inactivation of the shutoff gene (UL41) of herpes simplex virus types 1 and 2. J. Gen. Virol. **71:**2961–2967.
9. **Fort, P., L. Marty, M. Piechaczyk, S. el Sabrouty, C. Dani, P. Jeanteur, and J. M. Blanchard.** 1985. Various rat adult tissues express only one major mRNA species from the glyceraldehyde-3-phosphate-dehydrogenase multigenic family. Nucleic Acids Res. **13:**1431–1442.
10. **Geiss, B. J., T. J. Smith, D. A. Leib, and L. A. Morrison.** 2000. Disruption of virion host shutoff activity improves the immunogenicity and protective capacity of a replication-incompetent herpes simplex virus type 1 vaccine strain. J. Virol. **74:**11137–11144.
11. **Goldstein, D. J., and S. K. Weller.** 1988. An ICP6::*lacZ* insertional mutagen is used to demonstrate that the UL52 gene of herpes simplex virus type 1 is required for virus growth and DNA synthesis. J. Virol. **62:**2970–2977.
12. **Grau, D. R., R. J. Visalli, and C. R. Brandt.** 1989. Herpes simplex virus stromal keratitis is not titer-dependent and does not correlate with neurovirulence. Investig. Ophthalmol. Vis. Sci. **30:**2474–2480.
13. **Hill, T. M., R. K. Sinden, and J. R. Sadler.** 1983. Herpes simplex virus types 1 and 2 induce shutoff of host protein synthesis in Friend erythroleukemia cells. J. Virol. **45:**241–250.
14. **Jones, F. E., C. A. Smibert, and J. R. Smiley.** 1995. Mutational analysis of the herpes simplex virus virion host shutoff protein: evidence that vhs functions in the absence of other viral proteins. J. Virol. **69:**4863–4871.
15. **Karr, B. M., and G. S. Read.** 1999. The virion host shutoff function of herpes simplex virus degrades the 5′ end of a target mRNA before the 3′ end. Virology **264:**195–204.
16. **Landry, M. L., D. M. Myerson, and C. Bull.** 1992. Recurrent genital infection in the guinea pig: differences between herpes simplex types 1 and 2. Intervirology **34:**169–179.
17. **Leib, D. A., D. M. Coen, C. L. Bogard, K. A. Hicks, D. R. Yager, D. M. Knipe, K. L. Taylor, and P. A. Schaffer.** 1989. Immediate-early regulatory gene mutants define different stages in the establishment and reactivation of herpes simplex virus latency. J. Virol. **63:**759–768.
18. **Lu, P., F. E. Jones, H. A. Saffran, and J. R. Smiley.** 2001. Herpes simplex virus virion host shutoff protein requires a mammalian factor for efficient in vitro endoribonuclease activity. J. Virol. **75:**1172–1185.
19. **Morrison, L. A., and D. M. Knipe.** 1994. Immunization with replication-defective mutants of herpes simplex virus type 1: sites of immune intervention in pathogenesis of challenge virus infection. J. Virol. **68:**689–696.
20. **Pak, A. S., D. N. Everly, K. Knight, and G. S. Read.** 1995. The virion host shutoff protein of herpes simplex virus inhibits reporter gene expression in the absence of other viral gene products. Virology **211:**491–506.
21. **Rader, K. A., C. E. Ackland-Berglund, J. K. Miller, J. S. Pepose, and D. A. Leib.** 1993. In vivo characterization of site-directed mutations in the promoter of the herpes simplex virus type 1 latency-associated transcripts. J. Gen. Virol. **74:**1859–1869.
22. **Read, G. S., and N. Frenkel.** 1983. Herpes simplex virus mutants defective in the virion associated shutoff of host polypeptide synthesis and exhibiting abnormal synthesis of α (immediate-early) viral polypeptides. J. Virol. **46:**498–512.
23. **Read, G. S., B. M. Karr, and K. Knight.** 1993. Isolation of a herpes simplex virus type 1 mutant with a deletion in the virion host shutoff gene and identification of multiple forms of the vhs (UL41) polypeptide. J. Virol. **67:**7149–7160.
24. **Sambrook, J., E. F. Fritsch, and T. Maniatis.** 1989. Molecular cloning: a laboratory manual. Cold Spring Harbor Laboratory Press, Cold Spring Harbor, N.Y.
25. **Smibert, C. A., D. C. Johnson, and J. R. Smiley.** 1992. Identification and characterization of the virion-induced host shutoff product of herpes simplex virus gene UL41. J. Gen. Virol. **73:**467–470.
26. **Smith, T. J., C. E. Ackland-Berglund, and D. A. Leib.** 2000. Herpes simplex virus virion host shutoff (vhs) activity alters periocular disease in mice. J. Virol. **74:**3598–3604.
27. **Stanberry, L. R., D. M. Jorgenson, and A. J. Nahmias.** 1997. Herpes simplex viruses 1 and 2, p. 419–454. *In* A. S. Evans and R. A. Kaslow (ed.), Viral infections of humans: epidemiology & control, 4th ed. Plenum Medical Book Co., New York, N.Y.
28. **Stoddart, C., R. Cardin, J. Boname, W. Manning, G. Abenes, and E. Mocarski.** 1994. Peripheral blood mononuclear phagocytes mediate dissemination of murine cytomegalovirus. J. Virol. **68:**6243–6253.
29. **Strelow, L., T. Smith, and D. Leib.** 1997. The virion host shutoff function of herpes simplex virus type 1 plays a role in corneal invasion and functions independently of the cell cycle. Virology **231:**28–34.
30. **Strelow, L. I., and D. A. Leib.** 1995. Role of the virion host shutoff (vhs) of herpes simplex virus type 1 in latency and pathogenesis. J. Virol. **69:**6779–6786.
31. **Strelow, L. I., and D. A. Leib.** 1996. Analysis of conserved domains of UL41 of herpes simplex virus type 1 in virion host shutoff and pathogenesis. J. Virol. **70:**5665–5667.
32. **Sucato, G., A. Wald, E. Wakabayashi, J. Vieira, and L. Corey.** 1998. Evidence of latency and reactivation of both herpes simplex virus (HSV)-1 and HSV-2 in the genital region. J. Infect. Dis. **177:**1069–1072.
33. **Tigges, M. A., S. Leng, D. C. Johnson, and R. L. Burke.** 1996. Human herpes simplex virus (HSV)-specific CD8+ CTL clones recognize HSV-2-infected fibroblasts after treatment with IFN-γ or when virion host shutoff functions are disabled. J. Immunol. **156:**3901–3910.
34. **Walker, J., K. A. Laycock, J. S. Pepose, and D. A. Leib.** 1998. Postexposure vaccination with a virion host shutoff defective mutant reduces UV-B radiation-induced ocular herpes simplex virus shedding in mice. Vaccine **16:**6–8.
35. **Walker, J., and D. A. Leib.** 1998. Protection from primary infection and establishment of latency by vaccination with a herpes simplex virus type 1 recombinant deficient in the virion host shutoff (vhs) function. Vaccine **16:**1–5.